



JGP 100th Anniversary

# The contribution of voltage clamp fluorometry to the understanding of channel and transporter mechanisms

John Cowgill<sup>1,2</sup>  and Baron Chanda<sup>2,3</sup> 

**Key advances in single particle cryo-EM methods in the past decade have ushered in a resolution revolution in modern biology. The structures of many ion channels and transporters that were previously recalcitrant to crystallography have now been solved. Yet, despite having atomistic models of many complexes, some in multiple conformations, it has been challenging to glean mechanistic insight from these structures. To some extent this reflects our inability to unambiguously assign a given structure to a particular physiological state. One approach that may allow us to bridge this gap between structure and function is voltage clamp fluorometry (VCF). Using this technique, dynamic conformational changes can be measured while simultaneously monitoring the functional state of the channel or transporter. Many of the important papers that have used VCF to probe the gating mechanisms of channels and transporters have been published in the *Journal of General Physiology*. In this review, we provide an overview of the development of VCF and discuss some of the key problems that have been addressed using this approach. We end with a brief discussion of the outlook for this technique in the era of high-resolution structures.**

## Historical perspective

Along with the development of voltage clamp electrophysiology, the work by Hodgkin, Huxley, and others established that changes in specific ion permeabilities were responsible for electrical activity in neurons and other excitable cells (Hodgkin and Huxley, 1952). Developments in methods to measure activities of single channels and reconstitution of purified ion channels in lipid bilayers demonstrated that the observed ionic currents were due to proteinaceous channels (Hladky and Haydon, 1970; White and Miller, 1979; Hamill et al., 1981). Electron micrographs of the torpedo electrical organ provided a first look at the architecture of an ion channel and pushed the field toward a molecular view of channel function (Klymkowsky and Stroud, 1979; Brisson and Unwin, 1984). This was soon followed by cloning of the nicotinic acetylcholine receptor, uncovering the molecular identity of a channel for the first time (Noda et al., 1982). In the ensuing period, widespread use of molecular biology methods in combination with newly developed single-channel electrophysiology techniques led to new molecular insights regarding channel structure and function

(Stühmer et al., 1989; Hoshi et al., 1990). Typical electrophysiological recordings measure ionic currents and, therefore, report directly on the open state but not the closed states. While the nature of the closed-state transitions can be inferred from ionic current experiments to some extent, gating currents enable direct assessment of these closed voltage-dependent transitions (Armstrong and Bezanilla, 1973; Schneider and Chandler, 1973). However, neither gating nor ionic currents provide any information about the structural nature of these transitions, and hence, there is a need for alternative methods to probe these transitions.

Site-directed mutagenesis enabled perturbation of the primary sequence of recombinantly expressed channels, thereby allowing identification of key determinants of channel gating (Mishina et al., 1985; Stühmer et al., 1989). In 1992, Arthur Karlin and Myles Akabas introduced substituted cysteine accessibility mapping (SCAM) to probe changes in water accessibility during channel gating (Akabas et al., 1992). SCAM provides invaluable structural insights but has some limitations. First, cysteine accessibility informs only on structural changes that are

<sup>1</sup>Graduate Program in Biophysics, University of Wisconsin, Madison, WI; <sup>2</sup>Department of Neuroscience, University of Wisconsin, Madison, WI; <sup>3</sup>Department of Biomolecular Chemistry, University of Wisconsin, Madison, WI.

Correspondence to Baron Chanda: [chanda@wisc.edu](mailto:chanda@wisc.edu).

© 2019 Cowgill and Chanda. This article is distributed under the terms of an Attribution–Noncommercial–Share Alike–No Mirror Sites license for the first six months after the publication date (see <http://www.rupress.org/terms/>). After six months it is available under a Creative Commons License (Attribution–Noncommercial–Share Alike 4.0 International license, as described at <https://creativecommons.org/licenses/by-nc-sa/4.0/>).

accompanied by changes in solvent accessibility. Second, SCAM requires that modification of substituted cysteines elicits a clear change in a functional phenotype. Finally, SCAM does not provide any information about the underlying kinetics.

For over half a century, biophysicists have turned to fluorescence spectroscopy to shed light on protein function at a molecular scale (Weber, 1952). The high sensitivity of fluorescence and the ability to measure fluorescence signals in vivo offer significant advantages over other spectroscopic methods such as NMR or EPR spectroscopy. Fluorescence can also provide information about the nature of the chemical environment around the probe and its proximity to other fluorophores or quenchers (Lakowicz, 2013). Such measurements have been critical for studies on soluble proteins and even some membrane proteins, but up until the mid-1990s, fluorescence spectroscopy has seen little use in the ion channel field for reasons outlined below.

Biophysical studies using fluorescence generally require a fluorescent probe capable of reporting on structural changes. The fluorescent amino acid tryptophan is an excellent probe due to its high quantum yield and extinction coefficient. However, tryptophans are ubiquitous in the cell, which makes it difficult to attribute the signal to a specific location. Historically, the alternative was to label the side chains such as lysines and cysteines with reactive fluorophores, but all these approaches required purifying the protein of interest.

Purifying recombinant ion channels from the membrane is challenging, but even with a purified channel in hand, several obstacles must be overcome to extract useful information. For starters, using fluorescence to track conformational changes during channel gating requires reconstitution of the channel in a lipid bilayer and development of a method to drive the channel through its gating cycle. For voltage-gated ion channels there is an additional complication; they must be reinserted into a bilayer asymmetrically, as in the plasma membrane of a cell to obtain meaningful measurements. To circumvent these issues, the Isacoff laboratory developed VCF, a technique that allows simultaneous measurements of fluorescence signals and electrical currents from labeled ion channels (Mannuzzu et al., 1996). Soon thereafter, the Bezanilla laboratory modified this technique to measure rapid conformational changes (Cha and Bezanilla, 1997). These measurements have the additional advantage that they can be performed in a native environment without the need for protein isolation. In the last 20 years, VCF has evolved to become one of the most versatile techniques in the ion channel and transporter field.

### Development of VCF

VCF relies on the simple idea that the signals due to the conformational changes can be measured if they are synchronized with stimulus jumps. Thus, it gets around the problem of purification and reconstitution of a membrane protein by isolating the signals that are locked to the stimulus. Adequate controls are necessary to show that the stimulus does not elicit similar voltage-dependent fluorescence change in the wild-type channel when labeled with fluorophores. In some instances, nonspecific labeling of the protein of interest has to be reduced by mutating

the accessible cysteines. In their groundbreaking work, Mannuzzu et al. (1996) labeled Shaker channels with introduced cysteines on the extracellular end of the voltage-sensing fourth transmembrane segment (S4) with tetramethylrhodamine malimide (TMRM; Table 1). By coupling epifluorescence measurements with two-electrode voltage clamp (TEV) on *Xenopus* oocytes, they were able to spectroscopically monitor structural changes using fluorescence and directly correlate them to functional changes observed via electrophysiology. Shaker channels with TMRM labels on the extracellular end of S4 showed fluorescence quenching upon depolarization, while channels lacking cysteines showed no change in signal. These studies provided the first spectroscopic evidence for S4 movement during voltage gating.

### Modifications to VCF methodology

Cha and Bezanilla (1997) soon adapted this technique to the cut-open vaseline gap (COVG) voltage clamp configuration, with several modifications to the fluorescence detection setup. The faster clamp speed of COVG compared to the TEV enabled studies on fast gating channels such as the voltage-gated sodium channel (Cha et al., 1999). Additionally, they used two separate detectors for fluorescence emission, a photodiode for rapid detection of changes in fluorescence intensity and a spectrograph coupled to a charge-coupled device for collecting fluorescence emission spectra. As the wavelength of fluorescence emission is often highly dependent on the chemical environment around a fluorophore, the ability to measure emission spectra under voltage clamp enhanced the structural information extracted using VCF. Subsequently, they were also able to obtain information about protein dynamics by performing fluorescence anisotropy measurements under voltage clamp conditions (Cha and Bezanilla, 1998).

Standard labeling techniques provide limited access to the cytoplasmic space, therefore inside-facing residues were not probed in the initial studies. Zheng and Zagotta (2000) overcame these limitations by combining the fluorescence measurements with the versatility of patch clamp electrophysiology. Blunck et al. (2004) were able to expand this technique to mammalian expression systems using TIRF rather than epifluorescence. Wulf and Pless (2018) recently added several modifications to the patch clamp fluorometry (PCF) configuration, which greatly increased the signal-to-noise ratio. A digital micromirror device was used to selectively excite omega-shaped membrane at the tip of the patch pipette. In combination with a physical mask in front of the electron-multiplying charge-coupled device, they were able to obtain a 10-fold increase in fluorescence signal while simultaneously increasing the acquisition rate by 50 fold.

### Probing channel dynamics using VCF

Most of the early applications of VCF followed the design of Mannuzzu et al. (1996), labeling a channel of interest at specific locations to probe structural changes and dynamics during gating. In the Shaker potassium channel, a slow conformational change of the S4 helix was uncovered using VCF that followed the same time course as C-type inactivation (Loots and Isacoff,

Table 1. Cysteine-reactive probes used in VCF studies

Probe	Spectral properties	Usage notes	Example references
Monobromobimane	$\lambda_{\text{ex}} = 394 \text{ nm}$ $\lambda_{\text{em}} = 490 \text{ nm}$	Very small size compared with other probes allows labeling of less accessible locations with lower risk of structural perturbation. Near-UV excitation may cause aberrant photodamage.	Islas and Zagotta, 2006; Taraska et al., 2009
DPTA-Tb <sup>3+</sup>	$\lambda_{\text{ex}} = 328 \text{ nm}$ $\lambda_{\text{em}} = 492 \text{ or } 546 \text{ nm}$	Terbium chelate used in LRET studies. Reduced orientation-dependence of energy transfer makes it a more reliable reporter for distance changes than conventional fluorophores. Requires laser excitation in UV range.	Cha et al., 1999; Posson et al., 2005
Fluorescein	$\lambda_{\text{ex}} = 494 \text{ nm}$ $\lambda_{\text{em}} = 512 \text{ nm}$	Bright, environmentally sensitive fluorescent probe but has pH sensitivity in the physiological range (pKa = 6.4) and is prone to photobleaching.	Cha and Bezanilla, 1997; Dempski et al., 2006
Alexa Fluor 488 C5	$\lambda_{\text{ex}} = 493 \text{ nm}$ $\lambda_{\text{em}} = 516 \text{ nm}$	Bright fluorescent probe with low pH sensitivity in the physiological range. Lower environmental sensitivity of emission makes it less sensitive to conformational changes in absence of added quenchers.	Zheng and Zagotta, 2000; Bruening-Wright et al., 2007
Oregon Green	$\lambda_{\text{ex}} = 501 \text{ nm}$ $\lambda_{\text{em}} = 526 \text{ nm}$	Derivative of fluorescein with reduced pH sensitivity due to lower pKa (4.6) and lower rate of photobleaching. Emission is highly sensitive to calcium concentrations.	Cha and Bezanilla, 1997
PyMPO	$\lambda_{\text{ex}} = 415 \text{ nm}$ $\lambda_{\text{em}} = 570 \text{ nm}$	Environmentally sensitive probe whose linear shape makes it less bulky than alternatives such as fluorescein or tetramethyl rhodamine. Extended shape means probe reaches far from point of labeling.	Savalli et al., 2006; Vaid et al., 2008
Tetramethyl rhodamine	$\lambda_{\text{ex}} = 548 \text{ nm}$ $\lambda_{\text{em}} = 576 \text{ nm}$	Most commonly used probe with high environmental sensitivity and good photostability.	Mannuzzo et al., 1996; Cha and Bezanilla, 1997

DPTA, diethylenetriaminepentaacetic acid; PyMPO, 1-[3-(succinimidylloxycarbonyl)benzyl]-4-[5-(4-methoxyphenyl)-2-oxazolyl]pyridinium bromide.

1998, 2000). This was the first evidence that C-type inactivation is accompanied by a conformational change in the proximity of a voltage sensor. Similar studies have probed the movement of the voltage sensors for hERG (Smith and Yellen, 2002; Es-Salah-Lamoureux et al., 2010), EAG (Bannister et al., 2005), BK (Savalli et al., 2006), KCNQ (Osteen et al., 2010), and HCN channels (Bruening-Wright et al., 2007), improving the understanding of both the molecular movement and the kinetics underlying voltage-dependent activation of these channels (Tables 1, 2, and 3).

In voltage-gated sodium channels, VCF showed that voltage sensors of the four nonidentical domains move asynchronously (Chanda and Bezanilla, 2002). The time course of fluorescence of probes attached to the S4 on domains I–III are rapid and track channel opening kinetics, whereas those attached to domain IV move at a much slower rate, and their time course correlates with entry into the inactivated state (Fig. 1). Furthermore, these time-dependent changes in fluorescence correlate with movement of gating charge and show that the domain IV voltage sensor primarily accounts for the slow charge movement. Subsequent studies reveal that the activation of domain IV is both necessary and sufficient for channel activation and is associated with a short-lived second open state that precedes channel inactivation (Capes et al., 2013; Goldschen-Ohm et al., 2013). Similar asynchronous voltage sensor movements were observed in voltage-gated calcium channels, although their gating mechanism differs from the sodium channels (Pantazis et al., 2014).

Application of VCF extends far beyond the voltage-gated ion channel superfamily. The first ligand-gated ion channel probed with VCF was the GABA<sub>A</sub> receptor where Chang and Weiss

(2002) provided spectroscopic evidence for distinct conformational changes associated with binding of agonists, competitive antagonists, and allosteric antagonists. Studies with the Cys-loop family of receptors continued with the nicotinic acetylcholine receptor with which similar distinct mechanisms were observed for the agonist acetylcholine compared with the partial agonist epibatidine (Dahan et al., 2004). Pless et al. (2007) and Pless and Lynch (2009) mapped the differences in conformational changes elicited by glycine and the competitive antagonist strychnine in the glycine receptor. Zheng and Zagotta (2000) used PCF to demonstrate conformational change in the C-linker region of CNG channels. Both VCF and PCF approaches have been applied to probe the dynamics of acid-sensing ASIC ion channels during gating (Passero et al., 2009; Wulf and Pless, 2018).

Numerous transporters have been probed using VCF as well. The first was the Na<sup>+</sup>/glucose transporter by the Wright group in 1998, monitoring voltage-dependent conformational changes in the active site of the transporter (Loo et al., 1998). In the Na<sup>+</sup>/K<sup>+</sup>-ATPase, VCF has been used to monitor voltage- and ion-dependent conformational changes in the  $\alpha$ ,  $\beta$ , and  $\gamma$  subunits to better understand the conformational dynamics during the transport cycle (Geibel et al., 2003; Dempski et al., 2006, 2008; Dürr et al., 2008). Larsson et al. (2004) used VCF to monitor conformational changes in the glutamate transporter associated with ligand and/or ion binding, as well as changes in membrane potential, enabling them to construct a detailed kinetic model for transport turnover. Several other neurotransmitter transporters have been examined in a similar fashion (Li et al., 2000; Li and Lester, 2002). VCF has even enabled study of nonelectrogenic transporters such as the H<sup>+</sup>/K<sup>+</sup>-ATPase (Dürr et al., 2008).

Table 2. Exogenous probes used in VCF studies

Probe	Usage notes	References
Toxins	Toxins often have highly specific binding sites that remain static during channel gating and therefore can serve as useful reference points for FRET studies. However, not all channels have highly specific toxins, and toxin binding can influence channel gating in some instances.	Posson et al., 2005; Kubota et al., 2017
DPA	Hydrophobic, anionic dye that rapidly localizes to the outer membrane leaflet at depolarized potentials and inner leaflet at hyperpolarized potentials. Often used in FRET studies probing distance changes relative to the membrane; however, it is known to modify channel gating for many ligand-gated ion channels.	Chanda et al., 2005; Taraska and Zagotta, 2007
Oxonol	Voltage-dependent, anionic dye that translocates between leaflets depending on membrane potential, similar to DPA. However, rate of translocation is on the order of hundreds of milliseconds, 350-fold slower than that of DPA.	Chanda et al., 2005
C18-NTA	Lipid mimetic with metal chelating tag at head group that can be used to label membrane with transition metals for probing distance changes relative to membrane.	Aman et al., 2016
Potassium iodide	Collisional quencher that is often used to probe changes in solvent accessibility during channel gating.	Mannuzzu et al., 1996; Zheng and Zagotta, 2000

NTA, nitrilotriacetic acid.

Much of the focus of VCF has been to describe the conformational changes underlying protein function. However, the VCF technique can also be used to provide other information about the mechanisms such as the energetics of coupling between two allosteric domains of an ion channel (Chowdhury and Chanda, 2010). Muroi et al. (2010) found that certain mutations have a singular effect on the voltage dependence of pore

conductance and voltage-sensor fluorescence. They shift the midpoints of G-V and F-V (fluorescence-voltage) curves in opposite directions. Analysis of allosteric models shows that these mutations disrupt a subset of coupling interactions between voltage-sensor and pore modules (These mutations, also known as class II interactors, disrupt conserved interactions that occur in both activated and resting state but not in intermediate states;

Table 3. Genetically incorporated probes used in VCF studies

Probe	Incorporation method	Usage notes	References
Tryptophan	Standard mutagenesis	Environmentally sensitive, naturally fluorescent amino acid that can also serve as a fluorescence quencher at distances >15 Å.	Islas and Zagotta, 2006; Pantazis et al., 2014
Lanthanide binding tag	Short tag sequence (DYNKDGWYEELE)	Used to chelate lanthanides for distance measurements with LRET. Requires labeling with micromolar concentrations of Tb <sup>3+</sup> .	Castillo et al., 2016; Carrasquel-Ursulaez et al., 2018
Fluorescent proteins	Tagging with numerous available protein sequences	Commonly used in protein-protein interaction or domain rearrangements FRET studies. Large number of fluorescent proteins allow tuning of spectral properties (GFP, YFP, CFP, mCherry, Citrine, etc.) although tags are very large (>20 kD), limiting use.	Siegel and Isacoff, 1997; Miranda et al., 2013
Halo tag	Tagging with a 295-amino acid sequence	Labeling achieved by incubation with Halo-specific label, with a wide range of labels available. Usage and limitations are similar to those of fluorescent proteins due to the large size.	Not used to date
SNAP tag	Tagging with a 182-amino acid sequence	Similar to Halo tag, with slightly smaller tag sequence (~33 kD compared with 19.4 kD).	Not used to date
Dihistidine motif	Introduction of two histidines into helical segment (HXXH or HXXXH)	Coordinates transition metals for use as fluorescence quenchers for use in transition metal FRET to probe distance changes at short range (>20 Å).	Taraska et al., 2009; Dai and Zagotta, 2017
ANAP	Nonsense codon suppression	Small, environmentally sensitive fluorescent unnatural amino acid introduced into <i>Xenopus</i> oocytes by inserting Amber stop codon (TAG) and coinjecting with nonsense suppressor tRNA and ANAP-tRNA synthetase.	Kalstrup and Blunck, 2013, 2018
Coumarin	Nonsense codon suppression	Small, environmentally fluorescent unnatural amino acid similar to ANAP. Has been used in HEK cells via cotransfection of nonsense suppressor tRNA and coumarin-tRNA synthetase, and gene of interest with TAG codon inserted.	Steinberg et al., 2017

SNAP, S-nitroso-N-acetylpenicillamine.

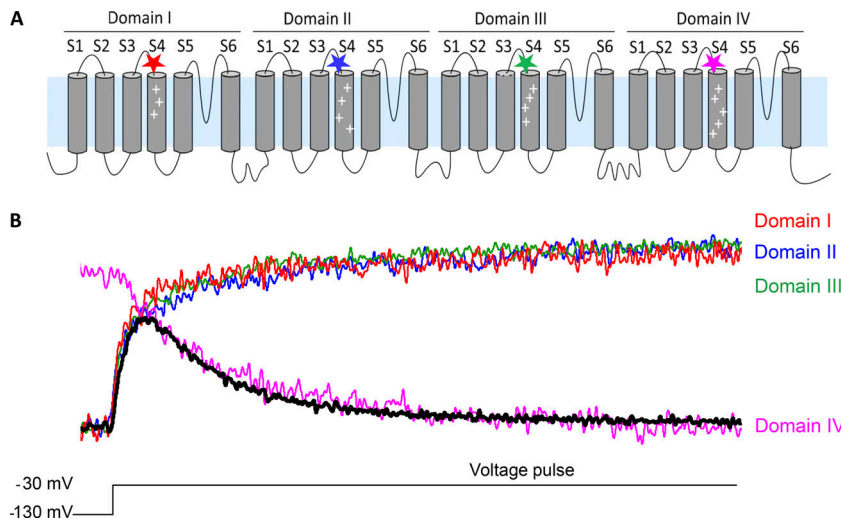


**Figure 1. VCF highlights the unique role of the sodium channel's domain IV voltage sensor.** (A) Membrane topology of a voltage-gated sodium ion channel. The location of the fluorescent probes on each of the S4s are highlighted using colored stars. (B) Comparison of the fluorescence response from each of the four domains of the sodium channel with ionic currents (black) in response to a depolarizing voltage pulse. The fluorescence response from the S4s of domains I, II, and III correlate with the activation of sodium channel. The domain IV fluorescence signal was inverted to highlight the tight correlation between sodium channel inactivation and domain IV activation kinetics. Note that these fluorescence kinetics were remarkably consistent over multiple positions in the same S4 segment. Ionic currents were obtained in the absence of external sodium and therefore represent efflux of internal potassium ions through the sodium channel. Adopted from [Chanda and Bezanilla \(2002\)](#).

class I interactors are observed only in the activated or resting state; see [Muroi et al., 2010](#)). In the rat skeletal muscle sodium channel, it was shown that residues in the S4-S5 linker of domain III are involved in such class II interactions. The Blunck group used a similar approach to show that the voltage-sensor mode shift observed in the Shaker potassium channel is due to voltage-sensor pore coupling, which is mediated by residues in the S4-S5 linker ([Haddad and Blunck, 2011](#)). More recently, the same approach was used to characterize allosteric coupling interactions in the KCNQ channel ([Zaydman et al., 2013](#)).

### Defining structural constraints by VCF-FRET

With the emergence of high-resolution structures of different ion channels at the turn of the century, our models of channel gating and function became increasingly sophisticated. In the early days, fluorescence intensity changes and spectral characteristics of the attached probes were used to interpret the nature of conformational changes in VCF experiments, but it became abundantly clear that the real potential lies in its ability to track specific structural changes in real time.

One of the prevailing questions in the field during this time was, how far does the S4 helix move during voltage activation? VCF was quickly adapted to address this issue by taking advantage of the exquisite sensitivity of FRET, which, under the right circumstances, can measure subnanometer distance changes. FRET occurs when energy from the excited state of one fluorophore (donor) is transferred to another (acceptor) via dipolar coupling, regenerating the ground state of the donor while simultaneously exciting the electrons in the acceptor molecule. The efficiency of this transfer is dependent on the spectral overlap, relative orientation, and distance between donor and acceptor as well as the refractive index of the environment. The spectral overlap and refractive index terms are generally constant for a given donor-acceptor pair in an experiment. Assuming that orientation of the donor and acceptor dipoles relative to each other is highly dynamic, FRET efficiency can be directly related to the distance between the donor and the acceptor. The FRET efficiency is inversely proportional to the sixth power of the distance, making it extremely sensitive to

changes in distance near the Förster radius ( $R_0$ ) of the donor-acceptor pair.

The Bezanilla and Isacoff laboratories were the first to exploit resonance energy transfer as a means to derive subnanometer measurements of conformational change using VCF. [Cha et al. \(1999\)](#) monitored energy transfer from a  $Tb^{3+}$  chelate to fluorescein labeled at identical sites on the voltage sensor of Shaker potassium channel. Due to the long-lived excited state of  $Tb^{3+}$ , this is called luminescence resonance energy transfer (LRET), and the efficiency is extracted by measuring the  $Tb^{3+}$  excited state lifetime in the presence of the acceptor. [Glauner et al. \(1999\)](#) used conventional FRET between a fluorescein donor and a TMRM acceptor to monitor intersubunit distance change. In their study, FRET efficiency was determined through changes in the donor photobleaching rate in the absence versus presence of acceptor. The closer the pair, the more energy is transferred from the donor, leading to a slower photobleaching rate.

Once the structure of the voltage-sensitive prokaryotic KVAP channel became available, two separate FRET experiments probed the paddle model in a functional channel. [Chanda et al. \(2005\)](#) used a dipicrylamine (DPA), an anionic lipophilic dye that redistributes between the inner and outer leaflet depending on the membrane potential. By monitoring FRET efficiency from DPA to rhodamine attached to the S4 helix of the Shaker potassium channel, they were able to demonstrate that the voltage-sensing paddle does not translocate across the membrane, as had been suggested at the time ([Jiang et al., 2003](#)). [Posson et al. \(2005\)](#) further constrained the movement of S4 using fluorescently labeled pore blockers as static reference points. The FRET between labels on S4 and pore blockers constrained the movement of S4 upon activation to  $<10 \text{ \AA}$  vertical displacement. Although multiple other approaches have been used to address this problem, the  $\sim 10\text{-\AA}$  movement remains the consensus view ([Swartz, 2008](#)) and is consistent with later structures of the resting voltage-sensing domain ([Li et al., 2014](#)).

### Defining structural constraints using alternative strategies

Since the early work on the Shaker potassium channel, DPA and fluorescently labeled toxins have been used to probe stimulus-

induced conformational changes in other channels (Table 2). DPA has been used for FRET-based structural studies in CNG (Taraska and Zagotta, 2007), TRP (De-la-Rosa et al., 2013), and AMPA (Zachariassen et al., 2016) channels as well the Ci-VSP (Sakata et al., 2016). However, DPA has been reported to modulate gating of channels like the GABA<sub>A</sub> (Chisari et al., 2011) and NMDA (Linsenbardt et al., 2013) receptors, precluding its use in structure–function studies of those channels. Fluorescently labeled toxin approaches have been used in the sodium channel (Kubota et al., 2017) and BK channel (Castillo et al., 2016; Carrasquel-Ursulaez et al., 2018), but many channels lack a specific blocker capable of tightly binding the pore without perturbing channel gating.

In 2009, the Zagotta laboratory introduced a new labeling strategy capable of labeling multiple sites with additional advantages over the existing approaches (Taraska et al., 2009). They engineered dihistidine motifs which bind to transition metal ions such as Ni<sup>2+</sup> or Cu<sup>2+</sup> and quench these fluorophores in a strongly distance-dependent manner analogous to traditional FRET. This can be used in combination with traditional cysteine-based labeling strategies to enable incorporation of two probes independently. The primary advantage of transition metal ion FRET is that it is able to measure changes over a much shorter distance compared to conventional FRET probes. Most commonly used FRET pairs have Förster radii of 45–70 Å, which means that the probes must be at this distance to achieve maximum sensitivity to distance changes. The Förster radii of Ni<sup>2+</sup> and Cu<sup>2+</sup> are 12 and 16 Å for FRET from fluorescein, respectively, making them much more suitable for short-range distance measurements. This approach was originally developed for labeling purified proteins but has been used extensively in VCF experiments.

Transition metal ion FRET and LRET enables the detection of subtle conformational changes at a close range using a broadly applicable labeling strategy. As VCF has evolved to detect a more nuanced angstrom-level movements, some of the caveats associated with these approaches should be considered. Transition metal probes can have long excited-state lifetimes (microseconds compared to nanoseconds for organic fluorophores), which skews the estimates toward shorter distances if the structure is highly dynamic. On the other hand, long lifetimes of the transition metal allows the donor (or acceptor) fluorophore to sample all possible orientations, which significantly reduces errors associated with the orientation term in the Förster equation. One should also take into account that some of the probes such as fluorescein and TMR are more than three times the size of a typical amino acid and, therefore, are not suitable for estimating small distance changes. One solution is to use cys-reactive bimanes (Kosower et al., 1979) as fluorescent labels in VCF (Islas and Zagotta, 2006; Taraska et al., 2009), but these dyes have inferior spectral characteristics.

An alternative strategy is to exploit the Dexter energy transfer mechanism to estimate distance changes over a very short distance range. This type of nonradiative energy transfer occurs within a distance of 10 Å and involves electron exchange between donor and acceptor pairs that have spectral overlap. For instance, rhodamine fluorescence can be quenched by

tryptophan by this mechanism (Cha and Bezanilla, 1998) and has been used to obtain distance restraints in the BK channel (Savalli et al., 2006). A variation of this approach involves the use of variable-length tethered quencher to estimate the distance between the anchoring site and a fluorescent probe attached to another part of the protein (Jarecki et al., 2013; Pantazis et al., 2014). In this approach, the distance between the probe and the anchoring site can be estimated in real time by monitoring the length dependence of quenching efficiency (Blaustein et al., 2000).

One of the inherent pitfalls of cysteine-based labeling is that it requires the attachment site to be accessible to externally applied reagents. Residues that are membrane-facing or buried in the protein interior cannot be probed using conventional VCF labeling techniques. The first genetic incorporation of fluorophores (Table 3) started with naturally occurring fluorescent protein, GFP. Siegel and Isacoff (1997) realized the potential of fluorescent proteins in VCF studies, fusing GFP to the C-terminus of Shaker, and showed that a voltage-dependent change in fluorescence correlated with movement of gating charges. By directly incorporating a fluorophore in the gene of interest, the nonspecific labeling that is inherent to cysteine-based strategies is eliminated, greatly improving the specific signal relative to the background. Furthermore, the cysteine-based approach generally requires removing all accessible endogenous cysteines, which can lead to misfolded protein or reduced expression. The growing library of fluorescent proteins with varying spectral properties quickly opened the door to FRET-based studies, as multiple fluorophores could be directly incorporated at distinct sites within a single gene or multiple genes. Zheng et al. (2003) used calmodulin fused to enhanced CFP with CNG channels labeled by eYFP to show dynamic association during channel gating using FRET. The Trudeau laboratory has used a similar approach to demonstrate association and rearrangement of the soluble domains in hERG channels (Gustina and Trudeau, 2009, 2013; Gianulis et al., 2013; Coddling and Trudeau, 2019). Fluorescent protein labeling has also been used in combination with DPA to map structural movements of soluble domains relative to the membrane in CNG (Taraska and Zagotta, 2007) and TRP channels (De-la-Rosa et al., 2013), as well as AMPA receptors (Zachariassen et al., 2016).

The primary challenge to using fluorescent proteins in VCF studies is their large size (~27 kD), which greatly restricts where proteins can be inserted without disrupting the structure. To minimize such perturbations, these probes are typically introduced at the N- or C-termini. Sheridan et al. (2002) developed an in vitro transposon-based method to randomly insert eGFP into the protein of interest and then screen for expression using surface fluorescence. Using this approach, Giraldez et al. (2005) identified permissible sites in the BK channel, which were later used to probe structural rearrangements in the RCK domain upon calcium and voltage activation of the channel (Miranda et al., 2013, 2016, 2018). Interestingly, some of the viable insertions were in highly structured regions, suggesting that ion channels may be more tolerant to large insertions than previously anticipated.

In 1989, the Schultz laboratory exploited a loophole in the genetic code to incorporate unnatural amino acids (uAAs) in a site-specific manner for the first time (Noren et al., 1989). They introduced a variety of uAAs into  $\beta$ -lactamase by chemically ligating them to a tRNA that recognized the Amber stop codon (UAG). This strategy has been used to incorporate a variety of uAAs into various ion channels (Nowak et al., 1995; Pless et al., 2010), but it was not until 2013 that it was first paired with VCF. Kalstrup and Blunck (2013) incorporated the fluorescent uAA ANAP into the voltage-sensing domain of Shaker, showing that it reports on conformational change associated with voltage gating. Additionally, they combined ANAP labeling with conventional cysteine labeling, using two-color VCF to simultaneously monitor movement at two different positions. Using this approach, they showed correlated movements of S4 and that the pore precedes channel opening, which was not detectable using existing methods. More recently, they used two-color VCF to characterize the movement of the S4–S5 linker, which is responsible for coupling S4 movement to pore opening in a process known as electromechanical coupling (Kalstrup and Blunck, 2018). Soh et al. (2017) adopted this approach to study the structural changes and mechanisms of partial agonism in glycine receptors. Coumarin has been used as an alternative to ANAP in probing rearrangements in the pore of TRPV1 during capsaicin activation (Steinberg et al., 2017). However, this approach requires chemically ligating the uAA to the Amber stop codon tRNA in vitro as opposed to using an engineered amino acyl-tRNA synthetase.

Genetic incorporation of ANAP has also been combined with FRET studies in several channels. Aman et al. (2016) determined that the transition metal binding site is responsible for potentiation of CNG channels by showing fluorescence quenching of an ANAP residue incorporated in the C-linker region. FRET between ANAP and DPA in the membrane was used to show that activation of Ci-VSP does not involve vertical movement of the catalytic region of the phosphatase (Sakata et al., 2016). Recently, the mechanism of voltage-dependent potentiation of ELK channels was probed using FRET between ANAP at the intrinsic ligand-binding site and  $\text{Co}^{2+}$  coordinated to the cyclic nucleotide binding homology domain (Dai and Zagotta, 2017; Dai et al., 2018).

### Single-molecule electrophysiology combined with fluorescence spectroscopy

Single-molecule studies can provide unprecedented details about the dynamics that are typically difficult to extract in a model-independent manner from ensemble data. Fluorescence spectroscopy and voltage clamp represent two of the very few techniques capable of reporting activity at a single-molecule level. Naturally, there was an early push to combine both single-molecule approaches in VCF. In a proof-of-principle experiment, Ide et al. (2002) used fluorescence to track single channels and voltage clamp to illustrate single-channel events in the same artificial bilayer, although not simultaneously. Borisenko et al. (2003) reported the first simultaneous observation of single-molecule fluorescence and single-channel activity using gramicidin in bilayers. They showed that association

of monomers of Cy3- and Cy5-labeled gramicidin shown by FRET correlated with single-channel openings in some recordings but not in others. While there have been a few other reports of combined single-molecule FRET and single-channel recordings, none of them have been able to convincingly measure activity and FRET from the same molecule at the same time. This type of measurement is necessary to relate conformational heterogeneity with various functional modalities that are typically obscured in ensemble measurements. Some of the technical difficulties associated with combining these two single-molecule techniques have been reviewed recently elsewhere (Weatherill and Wallace, 2015)

### Concluding remarks

It is abundantly clear that the molecular details provided by high-resolution structural approaches such as cryo-EM and x-ray diffraction are unrivaled by currently available techniques. But the ability of VCF to simultaneously report on structure, dynamics, and function will allow us to annotate the numerous high-resolution structures that are emerging at an increasingly rapid pace. The readouts provided by VCF will help bring the static structures to life. It is now routine to measure activity and conformational change at the same time in a near-native environment for many ion channels and transporters. We envision that, in the near future, VCF will become an essential tool to complement existing electrophysiological and structural approaches for studying the mechanisms of ion channel gating and function.

### Acknowledgments

Olaf S. Andersen served as editor.

This work was supported by funding from the National Institutes of Health to B. Chanda (NS101723, GM 131662, NS081293) and J. Cowgill (T32 HL-07936-17) and a University of Wisconsin-Madison UW2020 award to B. Chanda.

The authors declare no competing financial interests.

### References

- Akabas, M.H., D.A. Stauffer, M. Xu, and A. Karlin. 1992. Acetylcholine receptor channel structure probed in cysteine-substitution mutants. *Science*. 258:307–310. <https://doi.org/10.1126/science.1384130>
- Aman, T.K., S.E. Gordon, and W.N. Zagotta. 2016. Regulation of CNGA1 Channel Gating by Interactions with the Membrane. *J. Biol. Chem.* 291: 9939–9947. <https://doi.org/10.1074/jbc.M116.723932>
- Armstrong, C.M., and F. Bezanilla. 1973. Currents related to movement of the gating particles of the sodium channels. *Nature*. 242:459–461. <https://doi.org/10.1038/242459a0>
- Bannister, J.P.A., B. Chanda, F. Bezanilla, and D.M. Papazian. 2005. Optical detection of rate-determining ion-modulated conformational changes of the ether-à-go-go K<sup>+</sup> channel voltage sensor. *Proc. Natl. Acad. Sci. USA*. 102:18718–18723. <https://doi.org/10.1073/pnas.0505766102>
- Blaustein, R.O., P.A. Cole, C. Williams, and C. Miller. 2000. Tethered blockers as molecular 'tape measures' for a voltage-gated K<sup>+</sup> channel. *Nat. Struct. Biol.* 7:309–311. <https://doi.org/10.1038/74076>
- Blunck, R., D.M. Starace, A.M. Correa, and F. Bezanilla. 2004. Detecting rearrangements of shaker and NaChBac in real-time with fluorescence spectroscopy in patch-clamped mammalian cells. *Biophys. J.* 86: 3966–3980. <https://doi.org/10.1529/biophysj.103.034512>
- Borisenko, V., T. Loughheed, J. Hesse, E. Füreder-Kitzmüller, N. Fertig, J.C. Behrends, G.A. Woolley, and G.J. Schütz. 2003. Simultaneous optical

- and electrical recording of single gramicidin channels. *Biophys. J.* 84: 612–622. [https://doi.org/10.1016/S0006-3495\(03\)74881-4](https://doi.org/10.1016/S0006-3495(03)74881-4)
- Brisson, A., and P.N.T. Unwin. 1984. Tubular crystals of acetylcholine receptor. *J. Cell Biol.* 99:1202–1211. <https://doi.org/10.1083/jcb.99.4.1202>
- Bruening-Wright, A., F. Elinder, and H.P. Larsson. 2007. Kinetic relationship between the voltage sensor and the activation gate in sPHCN channels. *J. Gen. Physiol.* 130:71–81. <https://doi.org/10.1085/jgp.200709769>
- Capes, D.L., M.P. Goldschen-Ohm, M. Arcisio-Miranda, F. Bezanilla, and B. Chanda. 2013. Domain IV voltage-sensor movement is both sufficient and rate limiting for fast inactivation in sodium channels. *J. Gen. Physiol.* 142:101–112. <https://doi.org/10.1085/jgp.201310998>
- Carrasquel-Ursulaez, W., O. Alvarez, F. Bezanilla, and R. Latorre. 2018. Determination of the Stoichiometry between alpha- and gamma 1 Subunits of the BK Channel Using LRET. *Biophys. J.* 114:2493–2497. <https://doi.org/10.1016/j.bpj.2018.04.008>
- Castillo, J.P., J.E. Sánchez-Rodríguez, H.C. Hyde, C.A. Zaelzer, D. Aguayo, R.V. Sepúlveda, L.Y.P. Luk, S.B.H. Kent, F.D. Gonzalez-Nilo, F. Bezanilla, and R. Latorre. 2016.  $\beta$ 1-subunit-induced structural rearrangements of the Ca<sup>2+</sup>- and voltage-activated K<sup>+</sup> (BK) channel. *Proc. Natl. Acad. Sci. USA.* 113:E3231–E3239. <https://doi.org/10.1073/pnas.1606381113>
- Cha, A., and F. Bezanilla. 1997. Characterizing voltage-dependent conformational changes in the Shaker K<sup>+</sup> channel with fluorescence. *Neuron.* 19: 1127–1140. [https://doi.org/10.1016/S0896-6273\(00\)80403-1](https://doi.org/10.1016/S0896-6273(00)80403-1)
- Cha, A., and F. Bezanilla. 1998. Structural implications of fluorescence quenching in the Shaker K<sup>+</sup> channel. *J. Gen. Physiol.* 112:391–408. <https://doi.org/10.1085/jgp.112.4.391>
- Cha, A., P.C. Ruben, A.L. George Jr., E. Fujimoto, and F. Bezanilla. 1999. Voltage sensors in domains III and IV, but not I and II, are immobilized by Na<sup>+</sup> channel fast inactivation. *Neuron.* 22:73–87. [https://doi.org/10.1016/S0896-6273\(00\)80680-7](https://doi.org/10.1016/S0896-6273(00)80680-7)
- Cha, A., G.E. Snyder, P.R. Selvin, and F. Bezanilla. 1999b. Atomic scale movement of the voltage-sensing region in a potassium channel measured via spectroscopy. *Nature.* 402:809–813. <https://doi.org/10.1038/45552>
- Chanda, B., and F. Bezanilla. 2002. Tracking voltage-dependent conformational changes in skeletal muscle sodium channel during activation. *J. Gen. Physiol.* 120:629–645. <https://doi.org/10.1085/jgp.20028679>
- Chanda, B., O.K. Asamoah, R. Blunck, B. Roux, and F. Bezanilla. 2005. Gating charge displacement in voltage-gated ion channels involves limited transmembrane movement. *Nature.* 436:852–856. <https://doi.org/10.1038/nature03888>
- Chang, Y., and D.S. Weiss. 2002. Site-specific fluorescence reveals distinct structural changes with GABA receptor activation and antagonism. *Nat. Neurosci.* 5:1163–1168. <https://doi.org/10.1038/nn926>
- Chisari, M., K. Wu, C.F. Zorumski, and S. Mennerick. 2011. Hydrophobic anions potentially and noncompetitively antagonize GABA(A) receptor function in the absence of a conventional binding site. *Br. J. Pharmacol.* 164(2b):667–680. <https://doi.org/10.1111/j.1476-5381.2011.01396.x>
- Chowdhury, S., and B. Chanda. 2010. Deconstructing thermodynamic parameters of a coupled system from site-specific observables. *Proc. Natl. Acad. Sci. USA.* 107:18856–18861. <https://doi.org/10.1073/pnas.1003609107>
- Codding, S.J., and M.C. Trudeau. 2019. The hERG potassium channel intrinsic ligand regulates N- and C-terminal interactions and channel closure. *J. Gen. Physiol.* 151:478–488.
- Dahan, D.S., M.I. Dibas, E.J. Petersson, V.C. Auyeung, B. Chanda, F. Bezanilla, D.A. Dougherty, and H.A. Lester. 2004. A fluorophore attached to nicotinic acetylcholine receptor beta M2 detects productive binding of agonist to the alpha delta site. *Proc. Natl. Acad. Sci. USA.* 101: 10195–10200. <https://doi.org/10.1073/pnas.0301885101>
- Dai, G., and W.N. Zagotta. 2017. Molecular mechanism of voltage-dependent potentiation of KCNH potassium channels. *eLife.* 6:e26355. <https://doi.org/10.7554/eLife.26355>
- Dai, G., Z.M. James, and W.N. Zagotta. 2018. Dynamic rearrangement of the intrinsic ligand regulates KCNH potassium channels. *J. Gen. Physiol.* 150: 625–635. <https://doi.org/10.1085/jgp.201711989>
- De-la-Rosa, V., G.E. Rangel-Yescas, E. Ladrón-de-Guevara, T. Rosenbaum, and L.D. Islas. 2013. Coarse architecture of the transient receptor potential vanilloid 1 (TRPV1) ion channel determined by fluorescence resonance energy transfer. *J. Biol. Chem.* 288:29506–29517. <https://doi.org/10.1074/jbc.M113.479618>
- Dempski, R.E., K. Hartung, T. Friedrich, and E. Bamberg. 2006. Fluorometric measurements of intermolecular distances between the alpha- and beta-subunits of the Na<sup>+</sup>/K<sup>+</sup>-ATPase. *J. Biol. Chem.* 281:36338–36346. <https://doi.org/10.1074/jbc.M60478200>
- Dempski, R.E., J. Lustig, T. Friedrich, and E. Bamberg. 2008. Structural arrangement and conformational dynamics of the gamma subunit of the Na<sup>+</sup>/K<sup>+</sup>-ATPase. *Biochemistry.* 47:257–266. <https://doi.org/10.1021/bi701799b>
- Dürr, K.L., N.N. Tavraz, D. Zimmermann, E. Bamberg, and T. Friedrich. 2008. Characterization of Na,K-ATPase and H,K-ATPase enzymes with glycosylation-deficient beta-subunit variants by voltage-clamp fluorometry in Xenopus oocytes. *Biochemistry.* 47:4288–4297. <https://doi.org/10.1021/bi800092k>
- Es-Salah-Lamoureaux, Z., R. Fougere, P.Y. Xiong, G.A. Robertson, and D. Fedida. 2010. Fluorescence-tracking of activation gating in human ERG channels reveals rapid S4 movement and slow pore opening. *PLoS One.* 5:e10876. <https://doi.org/10.1371/journal.pone.0010876>
- Geibel, S., J.H. Kaplan, E. Bamberg, and T. Friedrich. 2003. Conformational dynamics of the Na<sup>+</sup>/K<sup>+</sup>-ATPase probed by voltage clamp fluorometry. *Proc. Natl. Acad. Sci. USA.* 100:964–969. <https://doi.org/10.1073/pnas.0337336100>
- Gianulis, E.C., Q. Liu, and M.C. Trudeau. 2013. Direct interaction of eag domains and cyclic nucleotide-binding homology domains regulate deactivation gating in hERG channels. *J. Gen. Physiol.* 142:351–366. <https://doi.org/10.1085/jgp.201310995>
- Giraldez, T., T.E. Hughes, and F.J. Sigworth. 2005. Generation of functional fluorescent BK channels by random insertion of GFP variants. *J. Gen. Physiol.* 126:429–438. <https://doi.org/10.1085/jgp.200509368>
- Glauner, K.S., L.M. Mannuzzu, C.S. Gandhi, and E.Y. Isacoff. 1999. Spectroscopic mapping of voltage sensor movement in the Shaker potassium channel. *Nature.* 402:813–817. <https://doi.org/10.1038/45561>
- Goldschen-Ohm, M.P., D.L. Capes, K.M. Oelstrom, and B. Chanda. 2013. Multiple pore conformations driven by asynchronous movements of voltage sensors in a eukaryotic sodium channel. *Nat. Commun.* 4:1350. <https://doi.org/10.1038/ncomms2356>
- Gustina, A.S., and M.C. Trudeau. 2009. A recombinant N-terminal domain fully restores deactivation gating in N-truncated and long QT syndrome mutant hERG potassium channels. *Proc. Natl. Acad. Sci. USA.* 106: 13082–13087. <https://doi.org/10.1073/pnas.0900180106>
- Gustina, A.S., and M.C. Trudeau. 2013. The eag domain regulates hERG channel inactivation gating via a direct interaction. *J. Gen. Physiol.* 141: 229–241. <https://doi.org/10.1085/jgp.201210870>
- Haddad, G.A., and R. Blunck. 2011. Mode shift of the voltage sensors in Shaker K<sup>+</sup> channels is caused by energetic coupling to the pore domain. *J. Gen. Physiol.* 137:455–472. <https://doi.org/10.1085/jgp.201010573>
- Hamill, O.P., A. Marty, E. Neher, B. Sakmann, and F.J. Sigworth. 1981. Improved patch-clamp techniques for high-resolution current recording from cells and cell-free membrane patches. *Pflugers Arch.* 391:85–100. <https://doi.org/10.1007/BF00656997>
- Hladky, S.B., and D.A. Haydon. 1970. Discreteness of conductance change in bimolecular lipid membranes in the presence of certain antibiotics. *Nature.* 225:451–453. <https://doi.org/10.1038/225451a0>
- Hodgkin, A.L., and A.F. Huxley. 1952. Currents carried by sodium and potassium ions through the membrane of the giant axon of *Loligo*. *J. Physiol.* 116:449–472. <https://doi.org/10.1113/jphysiol.1952.sp004717>
- Hoshi, T., W.N. Zagotta, and R.W. Aldrich. 1990. Biophysical and molecular mechanisms of Shaker potassium channel inactivation. *Science.* 250: 533–538. <https://doi.org/10.1126/science.2122519>
- Ide, T., Y. Takeuchi, and T. Yanagida. 2002. Development of an Experimental Apparatus for Simultaneous Observation of Optical and Electrical Signals from Single Ion Channels. *Single Molecules.* 3:33–42. [https://doi.org/10.1002/1438-5171\(200204\)3:1<33::AID-SIMO33>3.0.CO;2-U](https://doi.org/10.1002/1438-5171(200204)3:1<33::AID-SIMO33>3.0.CO;2-U)
- Islas, L.D., and W.N. Zagotta. 2006. Short-range molecular rearrangements in ion channels detected by tryptophan quenching of bimane fluorescence. *J. Gen. Physiol.* 128:337–346. <https://doi.org/10.1085/jgp.200609556>
- Jarecki, B.W., S. Zheng, L. Zhang, X. Li, X. Zhou, Q. Cui, W. Tang, and B. Chanda. 2013. Tethered spectroscopic probes estimate dynamic distances with subnanometer resolution in voltage-dependent potassium channels. *Biophys. J.* 105:2724–2732. <https://doi.org/10.1016/j.bpj.2013.11.010>
- Jiang, Y., V. Ruta, J. Chen, A. Lee, and R. MacKinnon. 2003. The principle of gating charge movement in a voltage-dependent K<sup>+</sup> channel. *Nature.* 423:42–48. <https://doi.org/10.1038/nature01581>
- Kalstrup, T., and R. Blunck. 2013. Dynamics of internal pore opening in K(V) channels probed by a fluorescent unnatural amino acid. *Proc. Natl. Acad. Sci. USA.* 110:8272–8277. <https://doi.org/10.1073/pnas.1220398110>
- Kalstrup, T., and R. Blunck. 2018. S4-S5 linker movement during activation and inactivation in voltage-gated K<sup>+</sup> channels. *Proc. Natl. Acad. Sci. USA.* 115:E6751–E6759. <https://doi.org/10.1073/pnas.1719105115>



- Klymkowsky, M.W., and R.M. Stroud. 1979. Immunospecific identification and three-dimensional structure of a membrane-bound acetylcholine receptor from Torpedo californica. *J. Mol. Biol.* 128:319–334. [https://doi.org/10.1016/0022-2836\(79\)90091-3](https://doi.org/10.1016/0022-2836(79)90091-3)
- Kosower, N.S., E.M. Kosower, G.L. Newton, and H.M. Ranney. 1979. Bimane fluorescent labels: labeling of normal human red cells under physiological conditions. *Proc. Natl. Acad. Sci. USA.* 76:3382–3386. <https://doi.org/10.1073/pnas.76.7.3382>
- Kubota, T., T. Durek, B. Dang, R.K. Finol-Urdaneta, D.J. Craik, S.B.H. Kent, R.J. French, F. Bezanilla, and A.M. Correa. 2017. Mapping of voltage sensor positions in resting and inactivated mammalian sodium channels by LRET. *Proc. Natl. Acad. Sci. USA.* 114:E1857–E1865. <https://doi.org/10.1073/pnas.1700453114>
- Lakowicz, J.R. 2013. *Principles of Fluorescence Spectroscopy*. Springer, New York.
- Larsson, H.P., A.V. Tzingounis, H.P. Koch, and M.P. Kavanaugh. 2004. Fluorometric measurements of conformational changes in glutamate transporters. *Proc. Natl. Acad. Sci. USA.* 101:3951–3956. <https://doi.org/10.1073/pnas.0306737101>
- Li, M., and H.A. Lester. 2002. Early fluorescence signals detect transitions at mammalian serotonin transporters. *Biophys. J.* 83:206–218. [https://doi.org/10.1016/S0006-3495\(02\)75162-X](https://doi.org/10.1016/S0006-3495(02)75162-X)
- Li, M., R.A. Farley, and H.A. Lester. 2000. An intermediate state of the gamma-aminobutyric acid transporter GAT1 revealed by simultaneous voltage clamp and fluorescence. *J. Gen. Physiol.* 115:491–508. <https://doi.org/10.1085/jgp.115.4.491>
- Li, Q., S. Wanderling, M. Paduch, D. Medovoy, A. Singharoy, R. McGreevy, C.A. Villalba-Galea, R.E. Hulse, B. Roux, K. Schulten, et al. 2014. Structural mechanism of voltage-dependent gating in an isolated voltage-sensing domain. *Nat. Struct. Mol. Biol.* 21:244–252. <https://doi.org/10.1038/nsmb.2768>
- Linsenbardt, A.J., M. Chisari, A. Yu, H.J. Shu, C.F. Zorumski, and S. Mennerick. 2013. Noncompetitive, voltage-dependent NMDA receptor antagonism by hydrophobic anions. *Mol. Pharmacol.* 83:354–366. <https://doi.org/10.1124/mol.112.081794>
- Loo, D.D.F., B.A. Hirayama, E.M. Gallardo, J.T. Lam, E. Turk, and E.M. Wright. 1998. Conformational changes couple Na<sup>+</sup> and glucose transport. *Proc. Natl. Acad. Sci. USA.* 95:7789–7794. <https://doi.org/10.1073/pnas.95.13.7789>
- Loots, E., and E.Y. Isacoff. 1998. Protein rearrangements underlying slow inactivation of the Shaker K<sup>+</sup> channel. *J. Gen. Physiol.* 112:377–389. <https://doi.org/10.1085/jgp.112.4.377>
- Loots, E., and E.Y. Isacoff. 2000. Molecular coupling of S4 to a K(+) channel's slow inactivation gate. *J. Gen. Physiol.* 116:623–636. <https://doi.org/10.1085/jgp.116.5.623>
- Mannuzzu, L.M., M.M. Moronne, and E.Y. Isacoff. 1996. Direct physical measure of conformational rearrangement underlying potassium channel gating. *Science.* 271:213–216. <https://doi.org/10.1126/science.271.5246.213>
- Miranda, P., J.E. Contreras, A.J. Plested, F.J. Sigworth, M. Holmgren, and T. Giraldez. 2013. State-dependent FRET reports calcium- and voltage-dependent gating-ring motions in BK channels. *Proc. Natl. Acad. Sci. USA.* 110:5217–5222. <https://doi.org/10.1073/pnas.1219611110>
- Miranda, P., T. Giraldez, and M. Holmgren. 2016. Interactions of divalent cations with calcium binding sites of BK channels reveal independent motions within the gating ring. *Proc. Natl. Acad. Sci. USA.* 113:14055–14060. <https://doi.org/10.1073/pnas.1611415113>
- Miranda, P., M. Holmgren, and T. Giraldez. 2018. Voltage-dependent dynamics of the BK channel cytosolic gating ring are coupled to the membrane-embedded voltage sensor. *eLife.* 7:e40664. <https://doi.org/10.7554/eLife.40664>
- Mishina, M., T. Tobimatsu, K. Imoto, K. Tanaka, Y. Fujita, K. Fukuda, M. Kurasaki, H. Takahashi, Y. Morimoto, T. Hirose, et al. 1985. Location of functional regions of acetylcholine receptor alpha-subunit by site-directed mutagenesis. *Nature.* 313:364–369. <https://doi.org/10.1038/313364a0>
- Muroi, Y., M. Arcisio-Miranda, S. Chowdhury, and B. Chanda. 2010. Molecular determinants of coupling between the domain III voltage sensor and pore of a sodium channel. *Nat. Struct. Mol. Biol.* 17:230–237. <https://doi.org/10.1038/nsmb.1749>
- Noda, M., H. Takahashi, T. Tanabe, M. Toyosato, Y. Furutani, T. Hirose, M. Asai, S. Inayama, T. Miyata, and S. Numa. 1982. Primary structure of alpha-subunit precursor of Torpedo californica acetylcholine receptor deduced from cDNA sequence. *Nature.* 299:793–797. <https://doi.org/10.1038/299793a0>
- Noren, C.J., S.J. Anthony-Cahill, M.C. Griffith, and P.G. Schultz. 1989. A general method for site-specific incorporation of unnatural amino acids into proteins. *Science.* 244:182–188. <https://doi.org/10.1126/science.2649980>
- Nowak, M.W., P.C. Kearney, J.R. Sampson, M.E. Saks, C.G. Labarca, S.K. Silverman, W. Zhong, J. Thorson, J.N. Abelson, N. Davidson, et al. 1995. Nicotinic receptor binding site probed with unnatural amino acid incorporation in intact cells. *Science.* 268:439–442. <https://doi.org/10.1126/science.7716551>
- Osteen, J.D., C. Gonzalez, K.J. Sampson, V. Iyer, S. Rebolledo, H.P. Larsson, and R.S. Kass. 2010. KCNE1 alters the voltage sensor movements necessary to open the KCNQ1 channel gate. *Proc. Natl. Acad. Sci. USA.* 107:22710–22715. <https://doi.org/10.1073/pnas.1016300108>
- Pantazis, A., N. Savalli, D. Sigg, A. Neely, and R. Olcese. 2014. Functional heterogeneity of the four voltage sensors of a human L-type calcium channel. *Proc. Natl. Acad. Sci. USA.* 111:18381–18386. <https://doi.org/10.1073/pnas.1411127112>
- Passero, C.J., S. Okumura, and M.D. Carattino. 2009. Conformational changes associated with proton-dependent gating of ASIC1a. *J. Biol. Chem.* 284:36473–36481. <https://doi.org/10.1074/jbc.M109.055418>
- Pless, S.A., and J.W. Lynch. 2009. Distinct conformational changes in activated agonist-bound and agonist-free glycine receptor subunits. *J. Neurochem.* 108:1585–1594. <https://doi.org/10.1111/j.1471-4159.2009.05930.x>
- Pless, S.A., M.I. Dibas, H.A. Lester, and J.W. Lynch. 2007. Conformational variability of the glycine receptor M2 domain in response to activation by different agonists. *J. Biol. Chem.* 282:36057–36067. <https://doi.org/10.1074/jbc.M706468200>
- Pless, S.A., J.D. Galpin, A. Frankel, and C.A. Ahern. 2010. A Cation-Pi Interaction in the Cardiac Sodium Channel Local Anesthetic Receptor Discriminates Between Antiarrhythmics. *Biophys. J.* 98:8a. <https://doi.org/10.1016/j.bpj.2009.12.048>
- Posson, D.J., P. Ge, C. Miller, F. Bezanilla, and P.R. Selvin. 2005. Small vertical movement of a K<sup>+</sup> channel voltage sensor measured with luminescence energy transfer. *Nature.* 436:848–851. <https://doi.org/10.1038/nature03819>
- Sakata, S., Y. Jinno, A. Kawanabe, and Y. Okamura. 2016. Voltage-dependent motion of the catalytic region of voltage-sensing phosphatase monitored by a fluorescent amino acid. *Proc. Natl. Acad. Sci. USA.* 113:7521–7526. <https://doi.org/10.1073/pnas.1604218113>
- Savalli, N., A. Kondratiev, L. Toro, and R. Olcese. 2006. Voltage-dependent conformational changes in human Ca(2+)- and voltage-activated K(+) channel, revealed by voltage-clamp fluorometry. *Proc. Natl. Acad. Sci. USA.* 103:12619–12624. <https://doi.org/10.1073/pnas.0601176103>
- Schneider, M.F., and W.K. Chandler. 1973. Voltage dependent charge movement of skeletal muscle: a possible step in excitation-contraction coupling. *Nature.* 242:244–246. <https://doi.org/10.1038/242244a0>
- Sheridan, D.L., C.H. Berlot, A. Robert, F.M. Inglis, K.B. Jakobsdottir, J.R. Howe, and T.E. Hughes. 2002. A new way to rapidly create functional, fluorescent fusion proteins: random insertion of GFP with an in vitro transposition reaction. *BMC Neurosci.* 3:7. <https://doi.org/10.1186/1471-2202-3-7>
- Siegel, M.S., and E.Y. Isacoff. 1997. A genetically encoded optical probe of membrane voltage. *Neuron.* 19:735–741. [https://doi.org/10.1016/S0896-6273\(00\)80955-1](https://doi.org/10.1016/S0896-6273(00)80955-1)
- Smith, P.L., and G. Yellen. 2002. Fast and slow voltage sensor movements in HERG potassium channels. *J. Gen. Physiol.* 119:275–293. <https://doi.org/10.1085/jgp.20028534>
- Soh, M.S., A. Estrada-Mondragon, N. Durisic, A. Keramidias, and J.W. Lynch. 2017. Probing the Structural Mechanism of Partial Agonism in Glycine Receptors Using the Fluorescent Artificial Amino Acid, ANAP. *ACS Chem. Biol.* 12:805–813. <https://doi.org/10.1021/acscchembio.6b00926>
- Steinberg, X., M.A. Kasimova, D. Cabezas-Bratesco, J.D. Galpin, E. Ladron-de-Guevara, F. Villa, V. Carnevale, L. Islas, C.A. Ahern, and S.E. Brauchi. 2017. Conformational dynamics in TRPV1 channels reported by an encoded coumarin amino acid. *eLife.* 6:e28626. <https://doi.org/10.7554/eLife.28626>
- Stühmer, W., F. Conti, H. Suzuki, X.D. Wang, M. Noda, N. Yahagi, H. Kubo, and S. Numa. 1989. Structural parts involved in activation and inactivation of the sodium channel. *Nature.* 339:597–603. <https://doi.org/10.1038/339597a0>
- Swartz, K.J. 2008. Sensing voltage across lipid membranes. *Nature.* 456:891–897. <https://doi.org/10.1038/nature07620>

- Taraska, J.W., and W.N. Zagotta. 2007. Structural dynamics in the gating ring of cyclic nucleotide-gated ion channels. *Nat. Struct. Mol. Biol.* 14: 854–860. <https://doi.org/10.1038/nsmb1281>
- Taraska, J.W., M.C. Puljung, and W.N. Zagotta. 2009. Short-distance probes for protein backbone structure based on energy transfer between bi-mane and transition metal ions. *Proc. Natl. Acad. Sci. USA.* 106: 16227–16232. <https://doi.org/10.1073/pnas.0905207106>
- Taraska, J.W., M.C. Puljung, N.B. Olivier, G.E. Flynn, and W.N. Zagotta. 2009a. Mapping the structure and conformational movements of proteins with transition metal ion FRET. *Nat. Methods.* 6:532–537. <https://doi.org/10.1038/nmeth.1341>
- Vaid, M., T.W. Claydon, S. Rezazadeh, and D. Fedida. 2008. Voltage clamp fluorimetry reveals a novel outer pore instability in a mammalian voltage-gated potassium channel. *J. Gen. Physiol.* 132:209–222. <https://doi.org/10.1085/jgp.200809978>
- Weatherill, E.E., and M.I. Wallace. 2015. Combining single-molecule imaging and single-channel electrophysiology. *J. Mol. Biol.* 427:146–157. <https://doi.org/10.1016/j.jmb.2014.07.007>
- Weber, G. 1952. Polarization of the fluorescence of macromolecules. I. Theory and experimental method. *Biochem. J.* 51:145–155. <https://doi.org/10.1042/bj0510145>
- White, M.M., and C. Miller. 1979. A voltage-gated anion channel from the electric organ of *Torpedo californica*. *J. Biol. Chem.* 254:10161–10166.
- Wulf, M., and S.A. Pless. 2018. High-Sensitivity Fluorometry to Resolve Ion Channel Conformational Dynamics. *Cell Reports.* 22:1615–1626. <https://doi.org/10.1016/j.celrep.2018.01.029>
- Zachariassen, L.G., L. Katchan, A.G. Jensen, D.S. Pickering, A.J.R. Plessted, and A.S. Kristensen. 2016. Structural rearrangement of the intracellular domains during AMPA receptor activation. *Proc. Natl. Acad. Sci. USA.* 113:E3950–E3959. <https://doi.org/10.1073/pnas.1601747113>
- Zaydman, M.A., J.R. Silva, K. Delaloye, Y. Li, H. Liang, H.P. Larsson, J. Shi, and J. Cui. 2013. Kv7.1 ion channels require a lipid to couple voltage sensing to pore opening. *Proc. Natl. Acad. Sci. USA.* 110:13180–13185. <https://doi.org/10.1073/pnas.1305167110>
- Zheng, J., and W.N. Zagotta. 2000. Gating rearrangements in cyclic nucleotide-gated channels revealed by patch-clamp fluorometry. *Neuron.* 28:369–374. [https://doi.org/10.1016/S0896-6273\(00\)00117-3](https://doi.org/10.1016/S0896-6273(00)00117-3)
- Zheng, J., M.D. Varnum, and W.N. Zagotta. 2003. Disruption of an inter-subunit interaction underlies Ca<sup>2+</sup>-calmodulin modulation of cyclic nucleotide-gated channels. *J. Neurosci.* 23:8167–8175. <https://doi.org/10.1523/JNEUROSCI.23-22-08167.2003>